Inorg. Chem. **2003**, *42*, 3891–3897

Electron Transfer through a Prenucleated Bimetalated Alanine-Based Peptide Helix

Kenneth J. Kise, Jr. and Bruce E. Bowler*

Department of Chemistry and Biochemistry, University of Denver, 2190 East Iliff Avenue, Denver, Colorado 80208-2436

Received November 8, 2002

We have synthesized a 22 residue alanine-based peptide with a tris(bipyridyl)ruthenium(II) amino acid near the middle of the peptide which can act as a photoinducible electron donor. Two histidines spaced *i*, *i* + 4 near the C-terminus of the peptide were then cross-linked with a tetraammineruthenium(III) moiety to prenucleate the helix and provide an electron acceptor site. Introduction of the cross-link enhances the average helix content from 67% to 84% at 0 °C, as judged by circular dichroism spectroscopy. The temperature dependence of the mean molar residue ellipticity at 222 nm, $[\Theta]_{222}$, for the bimetalated peptide was fit to a modified Lifson–Roig helix–coil model to permit extraction of the population of helical conformation at each residue separating the electron donor and acceptor. On average, the residues between the donor and acceptor are 92% helical. Photoinduced electron transfer with a driving force of –1.0 eV and an estimated reorganization energy of 0.82 eV was measured by fluorescence quenching methods in H_2O and D_2O, yielding rate constants, k_{ET}, of $7 \pm 3 \times 10^6$ s^{-1} and $5 \pm 1 \times 10^6$ s^{-1} at 0 °C. Calculation of the electronic coupling matrix element, H_{ab}, with the Marcus equation yields a value of 0.19 ± 0.4 cm^{-1}. Analysis in terms of the pathway model for electronic coupling indicates that this magnitude of H_{ab} is consistent with the participation of hydrogen bonds in electronic coupling for an isolated α-helix.

Introduction

Studies on electron transfer in model proteins have indicated that the details of the protein medium can have an important impact on the electronic coupling between the donor and acceptor.[1−3] Analysis of electronic coupling by the pathway model[1,2] indicates that the two common secondary structures, α-helix and *β*-sheet, should mediate electronic coupling with significantly different efficiencies. This partitioning of electronic coupling efficiency into α- and *β*-regions is supported by experiments on predominately α-helical[1,4] and *β*-sheet[5,6] proteins. However, the complications of tertiary interactions in proteins[1] make the pursuit of simple peptide models desirable to aid in delineating the effects of secondary structure on electronic coupling in proteins.

To this end, a number of peptide model systems have been developed to approach this problem. Metal-templated[7,8] and cyclic peptide-templated[9] de novo designed helix bundles have been prepared, as have coiled-coil peptides,[10−12] to serve as intramolecular donor−acceptor electron transfer model systems. These systems have the advantage of being structurally robust, but they still retain the complications of tertiary structure interactions in the electronic coupling medium. Several monomeric helix-forming peptides have also been studied,[13−17] although these peptides have generally been studied in nonaqueous solvents. These latter systems have, however, provided interesting insights into the electronic coupling properties of monomeric peptides, including directionality effects caused by the helix dipole,[13] and evidence for the unusual periodicity of electron transfer rates with

* Corresponding author. E-mail: bbowler@du.edu. Phone: 303-871-2985. Fax: 303-871-2254.

(1) Winkler, J. R.; Di Bilio, A. J.; Farrow, N. A.; Richards, J. H.; Gray, H. B. *Pure Appl. Chem.* **1999**, *71*, 1753−1764.
(2) Gray, H. B.; Winkler, J. R. *Annu. Rev. Biochem.* **1996**, *65*, 537−561.
(3) Onuchic, J. N.; Beratan, D. N.; Winkler, J. R.; Gray, H. B. *Annu. Rev. Biophys. Biomol. Struct.* **1992**, *21*, 349−377.
(4) Langen, R.; Colon, J. L.; Casimiro, D. R.; Karpishin, T. B.; Winkler, J. R.; Gray, H. B. *J. Biol. Inorg. Chem.* **1996**, *1*, 221−225.
(5) Langen, R.; Chang, I.-J.; Germanas, J. P.; Richards, J. H.; Winkler, J. R.; Gray, H. B. *Science* **1995**, *268*, 1733−1735.
(6) Regan, J. J.; Di Bilio, A. J.; Langen, R.; Skov, L. K.; Winkler, J. R.; Gray, H. B.; Onuchic, J. N. *Chem. Biol.* **1995**, *2*, 489−496.
(7) Mutz, M. W.; Case, M. A.; Wishart, J. F.; Ghadiri, M. R.; McLendon, G. L. *J. Am. Chem. Soc.* **1999**, *121*, 858−859.
(8) Zhou, J.; Case, M. A.; Wishart, J. F.; McLendon, G. L. *J. Phys. Chem. B* **1998**, *102*, 9975−9980.
(9) Rau, H. K.; DeJonge, N.; Haehnel, W. *Proc. Natl. Acad. Sci. U.S.A.* **1998**, *95*, 11526−11531.
(10) Kozlov, G. V.; Ogawa, M. Y. *J. Am. Chem. Soc.* **1997**, *119*, 8377−8378.
(11) Kornilova, A. Y.; Wishart, J. F.; Xiao, W.; Lasey, R. C.; Fedorova, A.; Shin, Y.-K.; Ogawa, M. Y. *J. Am. Chem. Soc.* **2000**, *122*, 7999−8006.
(12) Lee, H.; Faraggi, M.; Klapper, M. H. *Biochim. Biophys. Acta* **1992**, *1159*, 286−294.

10.1021/ic026166d CCC: $25.00
Published on Web 05/17/2003

sequence separation along an α-helix due to the mediation of electronic coupling by hydrogen bonds.[17] Other simple model systems have also demonstrated the importance of hydrogen bonding in mediating electron coupling between electron donors and acceptors.[18−20]

In this report, we describe the design, characterization, and electron transfer properties of a monomeric α-helical donor−acceptor compound which is soluble in aqueous solution. The system is based on the well-characterized alanine-based peptide helices developed by Baldwin and co-workers.[21] A number of considerations were important in the design of an electron transfer system using alanine-based helices. There has been some debate regarding the periodicity of alanine-based helices. Spin-labeling methods suggested a 3_{10}-helix structure,[22] although $J_{HN\alpha}$ coupling constants from NMR data are consistent with the central portions of these peptide helices having α-helical structure.[23] Deviations from α-helix structure appear to be localized toward the peptide N- and C-termini.[23] To deal with this ambiguity, we use histidines *i*, *i* + 4, at the C-terminus of our helical electron transfer peptide. These histidines are then cross-linked with a substitution inert tetraammineruthenium(III) moiety.[24] The role of this design element is threefold. It enforces the periodicity of the α-helix, as indicated by NMR data from studies on a cross-linked heptapeptide fragment.[25] It increases the overall stability of the helix[24,25] by prenucleating the helix and thus prevents fraying at the C-terminus. It also provides an electron acceptor site. Given observed directionality effects of the helix dipole for electron transfer along an α-helix,[13] it is also important to be able to control placement of the donor and acceptor along the helix. To this end, we developed a tris(bipyridyl)ruthenium(II) amino acid that could be incorporated into the peptide during solid phase peptide synthesis and serve as a photoinducible electron donor.[26] Our data on this amino acid show that it is compatible with helix formation, having a moderate helix propagation parameter, *w*, of 0.5 ± 0.1.[26] Use of a bipyridyl amino acid as a means to connect a tris(bipyridyl)ruthenium(II) photoinducible donor to a protein has also previously been shown to provide for much more efficient intramolecular electron transfer reactions in proteins relative to a bis(bipyridyl)ruthenium(II) moiety attached through a histidine side chain.[27] In this case, the bipyridyl anion radical of the excited state is directly coupled to the polypeptide backbone, rather than being centered on the outer bipyridyl rings as in attachment through histidine.[27] To be certain that electron transfer is through the helical structure, the tris(bipyridyl)ruthenium(II) amino acid is positioned near the center of the helix where fraying should be minimal. The tris(bipyridyl)ruthenium(II) amino acid is also spaced *i*, *i* + 5 from the nearest histidine of the electron acceptor site, so that the donor and acceptor will be on opposite faces of the helix. This placement minimizes the possibility of direct donor−acceptor contact. Lysines are spaced *i*, *i* + 5, to provide water solubility and to prevent peptide aggregation.[28] The sequence of the 22-residue peptide used is Ac-AKA-AAAKAAAABAAAAHAAAHA-$CONH_2$ (Ac is an acetyl capping group at the N-terminus of the peptide, A, K, and H are the one letter codes for alanine, lysine, and histidine, respectively, B represents the tris(bipyridyl)ruthenium(II) amino acid, and $CONH_2$ is a C-terminal carboxamide). The structure of the bimetalated electron transfer peptide, ET peptide, is presented schematically in Figure 1.

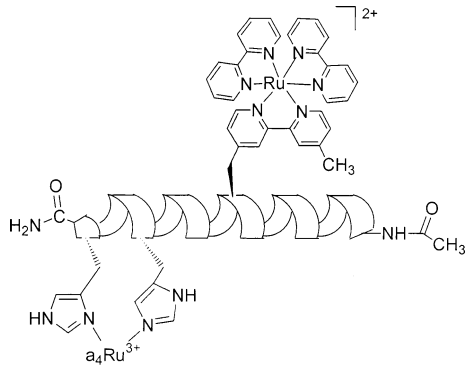

Figure 1. Schematic representation of the α-helical bimetalated electron transfer peptide (ET peptide). The ϵN/δN ligation to the two histidines, shown for the a_4Ru^{3+} moiety, is based on NMR data for a a_4Ru^{3+} cross-linked heptapeptide, Ac-AHAAAHA-$CONH_2$.[25]

In this paper, we present the synthesis of this helical donor−acceptor compound. We characterize the structure using circular dichroism (CD) methods as a function of temperature and analyze the data using a modified form of Lifson−Roig helix−coil theory, developed in this laboratory, to account for the effects of the prenucleating *i*, *i* + 4 cross-link.[25] Electron transfer data is acquired using fluorescence quenching methods in both H_2O and D_2O and the data interpreted in the context of existing data on intramolecular protein electron transfer reactions.

Experimental Section

Materials and Methods. As a general rule, all manipulations were done under low-light conditions. All chemicals were used as purchased. *cis*-Dichlorotetraammineruthenium(III) chloride, *cis*-[a_4-

(13) Galoppini, E.; Fox, M. A. *J. Am. Chem. Soc.* **1996**, *118*, 2299−2300.
(14) Sisido, M.; Tanaka, R.; Inai, Y.; Imanishi, Y. *J. Am. Chem. Soc.* **1989**, *111*, 6790−6796.
(15) Inai, Y.; Sisido, M.; Imanishi, Y. *J. Phys. Chem.* **1990**, *94*, 6237−6243.
(16) Inai, Y.; Sisido, M.; Imanishi, Y. *J. Phys. Chem.* **1991**, *95*, 3847−3851.
(17) Sisido, M.; Hoshino, S.; Kusano, H.; Kuraki, M.; Makino, M.; Sasaki, H.; Smith, T. A.; Ghiggino, K. P. *J. Phys. Chem. B* **2001**, *105*, 10407−10415.
(18) de Rege, P. J. F.; Williams, S. A.; Therien, M. J. *Science* **1995**, *269*, 1409−1413.
(19) Turró, C.; Chang, C. K.; Leroi, G. E.; Cukier, R. I.; Nocera, D. G. *J. Am. Chem. Soc.* **1992**, *114*, 4013−4015.
(20) Williamson, D. A.; Bowler, B. E. *J. Am. Chem. Soc.* **1998**, *120*, 10902−10911.
(21) Baldwin, R. L. *Biophys. Chem.* **1995**, *55*, 127−135.
(22) Milhauser, G. L. *Biochemistry* **1995**, *34*, 3873−3877.
(23) Milhauser, G. L.; Stenland, C. J.; Bolin, K. A.; van de Ven, F. J. M. *J. Biomol. NMR* **1996**, *7*, 331−334.
(24) Ghadiri, M. R.; Fernholz, A. K. *J. Am. Chem. Soc.* **1990**, *112*, 9633−9635.
(25) Kise, K. J., Jr.; Bowler, B. E. *Biochemistry* **2002**, *41*, 15826−15837.
(26) Kise, K. J., Jr.; Bowler, B. E. *Inorg. Chem.* **2002**, *41*, 379−386.
(27) Wuttke, D. S.; Gray, H. B.; Fisher, S. L.; Imperiali, B. *J. Am. Chem. Soc.* **1993**, *115*, 8455−8456.
(28) Chakrabartty, A.; Kortemme, T.; Baldwin, R. L. *Protein Sci.* **1994**, *3*, 843−852.

$RuCl_2$]Cl, and sodium (ethylenediaminetetraacetato)cobaltate(III), Co(EDTA), were prepared according to literature procedures.[29,30] The tris(bipyridyl)ruthenium(II) peptide, Ac-AKAAAAKAAAA-BAAAAHAAAHA-$CONH_2$ (RuBpy peptide), was prepared as described previously.[26] After the peptide was modified with *cis*-[a_4RuCl_2]Cl, it was purified by HPLC with a dual-pump system (Pharmacia), equipped with a VWM 2141 variable dual wavelength monitor (Pharmacia). A C18 reversed-phase analytical column (Vydac model number 218TP104) and a water/acetonitrile gradient were used for purification. MALDI-TOF mass spectra were acquired either in the laboratory of Dr. John Stewart, at the University of Colorado Health Sciences Center, or by Dr. Joe Hankin, at the School of Pharmacy, University of Colorado Health Sciences Center. Absorbance spectroscopy was done on a Beckman DU-640 spectrometer. Steady-state fluorescence was performed on a Spex Fluorolog 2 fluorimeter. CD measurements were done on a JASCO J500-C spectropolarimeter.

Modification of the RuBpy Peptide. *cis*-Dichlorotetraamminеruthenium(III) chloride (0.34 mg, 1.22×10^{-6} mol) was dissolved in 500 μL of Tris buffer (100 mM at pH 7). This solution was saturated with argon, to remove oxygen. In a separate flask, freshly made zinc amalgam (Zn/Hg) was also saturated with argon. The ruthenium solution was transferred by cannula onto the amalgam. This was stirred for 1 h under argon.

The RuBpy peptide (1 mg, 4.08×10^{-7} mol) was dissolved in 100 μL of the Tris buffer and saturated with argon. The reduced ruthenium tetraammine solution was transferred by cannula to the vial containing the peptide. This solution was stirred under argon for 4 h. Then, CoEDTA (1 mg, 2.45×10^{-6} mol) was added to the reaction to oxidize the ruthenium tetraammine back to the substitution inert 3+ oxidation state.

The bimetalated electron transfer peptide (ET peptide) was crudely purified using a CM-Sepharose column and ammonium chloride solutions as eluent. The CoEDTA was eluted from the column with 0.01 M NH_4Cl, as a purple band. For purposes of minimizing the amount of salt present with the peptide before the next purification step, it was eluted with 1 M HCl. The peptide was then lyophilized.

The final purification of the peptide was done by HPLC with a C18 reversed-phase analytical column, with a water/acetonitrile gradient at a flow rate of 1 mL/min. The mobile phase begins at 5% acetonitrile for 5 min, and then it goes to 50% acetonitrile at 45 min. The gradient is brought back down to 5% acetonitrile at 50 min, and then maintained at 5% acetonitrile until the end of the run (55 min). The ET peptide eluted at 28.75 min. Special care was taken when collecting the desired product, as it came off the column very soon after the starting RuBpy peptide (27.40 min).

Circular Dichroism. The peptide was dissolved in 800 μL of buffer (1 M NaCl, 1 mM sodium citrate, 1 mM sodium phosphate, 1 mM sodium borate) at a concentration of 3.92 μM. The sensitivity of the JASCO J500-C was set to 2 millidegree/cm, and the slit width was 1800 μm. Initially, the temperature was set to 0 °C, which was maintained by a Fisher Scientific model 9110 water bath (with a 1:1 water/ethylene glycol mixture). The temperature of the sample cell was monitored directly with a type T (copper−constantan) thermocouple (Digisense Thermocouple Thermometer, ColePalmer).

A wavelength scan was run initially from 325 to 200 nm. For the temperature denaturation, the ellipticity was measured at 300 nm (baseline) and at 222 nm (α-helix). The temperature was increased from 0 to 60 °C in 5 °C increments.

The data were converted from raw chart recorder deflection (cm) into mean molar ellipticity (degree cm^2 $dmol^{-1}$) with eq 1

$$[\Theta] = (M_r\psi(\text{sens}))/(100lc) \quad (1)$$

where M_r is the molecular weight of the compound, ψ is the raw chart recorder deflection (centimeters), sens is the sensitivity of the instrument in millidegrees per centimeter, l is the path length of the cell in decimeters (0.1 in our case), and c is the concentration in grams per liter. [Θ] is then divided by the number of residues in the peptide (22 in our case) to obtain the mean molar residue ellipticity at 222 nm, $[\Theta]_{222}$.

The $[\Theta]_{222}$ values were converted to fractional helicity using eq 2[31]

$$f_H = ([\Theta]_{222} - \Theta_C)/(\Theta_H - \Theta_C) \quad (2)$$

where Θ_H is the baseline ellipticity for a complete helix, and Θ_C is the baseline ellipticity for a random coil. The values for Θ_H and Θ_C as a function of temperature, T, are[31,32]

$$\Theta_H = (-44000 + 250T)(1 - x/N_r) \quad (3)$$

$$\Theta_C = 2220 - 53T \quad (4)$$

where N_r is the number of amino acid residues in the peptide. The value of −44000 is the per residue ellipticity for an infinite helix, and 2220 is the per residue value for a random coil, both at 0 °C in H_2O at 222 nm, and $x = 3$ accounts for helix end effects and is the number of non-hydrogen bonded carbonyl units at the C-terminus.[31,32]

The temperature dependence of $[\Theta]_{222}$ was fit to a modification of the Lifson−Roig helix−coil model that accounts for the effects of cross-links on helix nucleation and propagation.[25] The enthalpy of the propagation parameter was taken as −0.8 kcal/mol, as previously.[25] In the modified model,[25] the helix nucleation parameter, υ, for the three alanines within the Ru(III) cross-link is expected to be increased and was designated υ_{35}. The nucleation parameter for the histidines surrounding the cross-link, υ_{nHis}, was taken as the geometric mean of the standard nucleation parameter ($\upsilon^2 = 0.0013$)[31] and υ_{35}, such that $\upsilon_{nHis} = (\upsilon_{35}\upsilon)^{1/2}$. It was also shown that the propagation parameters for the nucleating alanines, w_{nAla}, and histidines, w_{nHis}, could be expressed as $w_{nAla} = w_{Ala} \times (\upsilon_{35}/\upsilon)$ and $w_{nHis} = w_{His} \times (\upsilon_{35}/\upsilon)^{1/2}$, where w_{Ala} and w_{His} are the standard propagation parameters reported for these amino acids in alanine-based peptide helices.[31] The standard nucleation parameter ($\upsilon^2 = 0.0013$) and propagation parameters, w, were used for all other amino acids in the peptide.[31] The propagation parameter derived from CD data for the tris(bipyridyl)ruthenium(III) amino acid ($w = 0.43$) was used.[26] Thus, the only adjustable parameter in fitting the temperature-dependent CD data for the ET peptide to the modified Lifson−Roig model was υ_{35}. Fractional helicities derived from the Lifson−Roig model were evaluated using matrix methods, as described previously.[25,26] The value of υ_{35} was adjusted to obtain the best fit between the experimental fractional helicities (eq 2) and the fractional helicities calculated from the Lifson−Roig model.

Steady-State Fluorescence. A Spex Fluorolog 2 fluorimeter was used for obtaining emission data. The spectra were obtained in water. The excitation wavelength was set at 450 nm, and emission was measured from 500 to 800 nm.

(29) Pell, S. D.; Sherban, M. M.; Tramontano, V.; Clarke, M. J. *Inorg. Synth.* **1989**, *26*, 65−68.
(30) Kirschner, S. *Inorg. Synth.* **1957**, *5*, 186−188.
(31) Rohl, C. A.; Baldwin, R. L. *Biochemistry* **1997**, *36*, 8435−8442.
(32) Luo, P.; Baldwin, R. L. *Biochemistry* **1997**, *36*, 8413−8421.

Lifetime Measurements. The peptide was dissolved in water or D_2O. The sample cell was set in a thermostated cell holder (Hitachi). The solution was maintained at 0 °C with a Fisher Scientific model 9110 water bath. The temperature was monitored with an electronic thermocouple. The sample was saturated with argon for 30 min before measuring the lifetime. A nitrogen/dye (Coumarin 120 dye in methanol) laser was used to excite the ET peptide. The laser excitation wavelength was set to 450 nm. The emission was monitored perpendicular to the laser excitation, through a monochromator set at 637 nm, and detected by a photomultiplier tube (PMT). The PMT was hooked up to a LeCroy 8013A A/D converter. The laser flashes were detected by a PMT set below the aperture of the laser. Twenty-five laser flashes were averaged for each individual lifetime measurement. The processing of the lifetime data was performed using Waveform Catalyst (LeCroy).

The raw data were converted from binary to ASCII before normalizing the data to the maximum fluorescence intensity in an Excel spreadsheet. The data were then imported into SigmaPlot (SSPS, Inc.), and fit to a double exponential decay curve (eq 5):

$$I(t) = I_1 e^{-t/\tau_1} + I_2 e^{-t/\tau_2} + I(\infty) \quad (5)$$

where $I(t)$ is the intensity of the emission at 637 nm, $I_1$and I_2 are the emission intensity amplitudes of the two decay processes, $I(\infty)$ is the final intensity at time $= \infty$, t is time, and τ_1 and τ_2 are the long and short emission lifetimes, respectively. Electron transfer rate constants, k_{ET}, are calculated from the short lifetime according eq 6, where τ_o is the lifetime of the tris(bipyridyl)ruthenium(II) excited state in the RuBpy peptide.

$$k_{ET} = 1/\tau_2 - 1/\tau_0 \quad (6)$$

Results and Discussion

Synthesis and Structural Characterization of the α-Helical Electron Transfer Peptide. The histidines separated i, $i + 4$ near the C-terminus of the peptide Ac-AKAAAA-KAAAABAAAAHAAAHA-NH_2 (RuBpy peptide) were cross-linked by reaction with substitution labile *cis*-dichlorotetraammineruthenium(II) chloride.[24,25] The product was oxidized with Co(EDTA) to produce the bis-ruthenium peptide (ET peptide) with a substitution inert *cis*-tetraammineruthenium(III) (a_4Ru^{3+}) cross-link of the histidines. The product was characterized by MALDI-TOF mass spectrometry. In the MALDI-TOF mass spectrum, the major peak was observed at 2550.4 *m*/*e*. This value is close to the mass expected for the product following loss of the four ammine ligands from the Ru(III) histidine cross-link (2551.8 *m*/*e*). Loss of all ammine ligands from ruthenium(III) metal complexes attached at histidines, during MALDI-TOF[33] or FAB[24] mass spectral measurements, has been noted previously. A small peak corresponding to the original peptide with no cross-link (expected, 2450.8 *m*/*e*, observed, 2450.0 *m*/*e*) was also observed. The peak at 2450 *m*/*e* became more prominent with repeated laser pulses from the MALDI-TOF mass spectrometer, indicating that the ET peptide was unstable to the conditions of MALDI-TOF mass spectral analysis.

In Figure 2, the CD spectrum of the a_4Ru^{3+} cross-linked peptide (ET peptide) is shown relative to the RuBpy peptide, which has no cross-link. The enhancement of helicity is clear from the distinct increase in mean molar residue ellipticity at 222 nm, $[\Theta]_{222}$, as well as from the increased ratio of negative ellipticity at 222 versus 208 nm. It is typical for the ratio $[\Theta]_{222}/[\Theta]_{208}$ to significantly exceed 1 for alanine-based peptides with high helical content.[34−36] The average fractional helicity of the ET peptide is increased to 0.84 (84%) from 0.67 (67%)[26] in the un-cross-linked RuBpy peptide. In Figure 3, the temperature dependence of ellipticity at 222 nm is shown. As expected, a substantial decrease in helical content occurs as temperature is increased. The solid

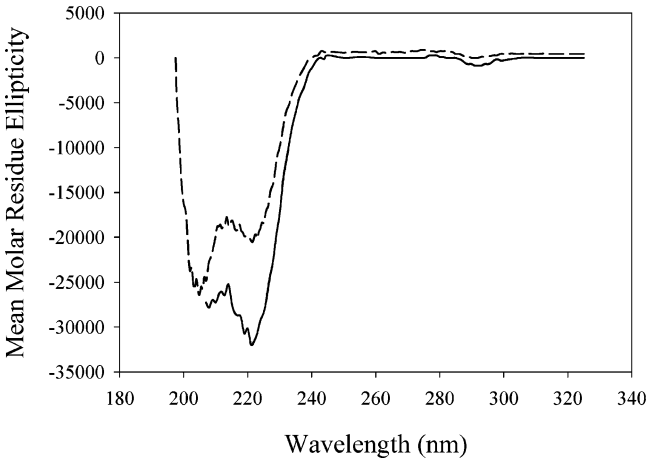

Figure 2. CD spectrum of the ET peptide (—) versus the CD spectrum of the RuBpy peptide (- - -). Spectra were obtained at 0 °C in 1 M NaCl, 1 mM sodium phosphate, 1 mM sodium citrate, 1 mM sodium borate, pH 7. The ET peptide was at a concentration of 3.92 μM. The RuBpy peptide was at a concentration of 9.44 μM. Mean molar residue ellipticity was evaluated as described in the Experimental Section.

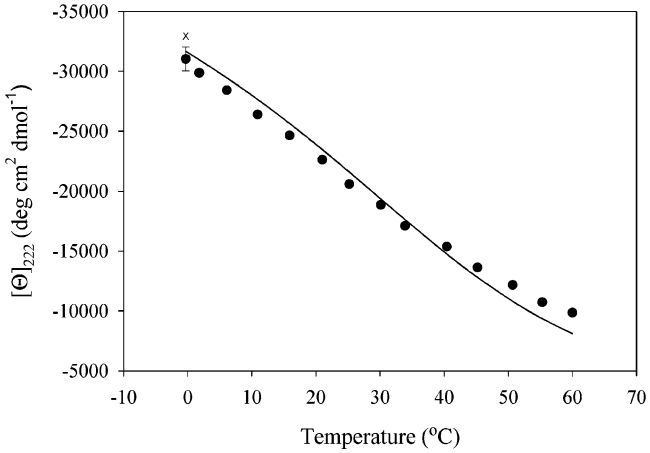

Figure 3. Temperature dependence of mean molar residue ellipticity at 222 nm, $[\Theta]_{222}$ (●), for the ET peptide. The peptide was dissolved in 1 M NaCl, 1 mM sodium phosphate, 1 mM sodium citrate, 1 mM sodium borate, pH 7. The ET peptide was at a concentration of 3.92 μM. The solid line (—) is a fit of the data to the modified Lifson−Roig helix−coil model described in the Experimental Section with $(\upsilon_{35})^2 = 0.0047$. The symbol, ×, at $T = 0$ °C shows the predicted $[\Theta]_{222}$ with $(\upsilon_{35})^2 = 0.009$ as found for a a_4Ru cross-linked heptapeptide.[25]

(33) Dahiyat, B. I.; Meade, T. J.; Mayo, S. L. *Inorg. Chim. Acta* **1996**, *243*, 207−212.

(34) Marqusee, S.; Robbins, V. H.; Baldwin, R. L. *Proc. Natl. Acad. Sci. U.S.A.* **1989**, *86*, 5286−5290.

(35) Marqusee, S.; Baldwin, R. L. *Proc. Natl. Acad. Sci. U.S.A.* **1987**, *84*, 8898−8902.

(36) Scholtz, J. M.; Marqusee, S.; Baldwin, R. L.; York, E. J.; Stewart, J. M.; Santoro, M.; Bolen, D. W. *Proc. Natl. Acad. Sci. U.S.A.* **1991**, *88*, 2854−2858.

line is a fit of the data to the modified Lifson−Roig helix−coil model described in the Experimental Section. The best fit to the model is obtained with the nucleation parameter, $(\upsilon_{35})^2$, resulting from the a_4Ru cross-link of histidines 17 and 21, set to 0.0047. This value is somewhat less than the value of 0.009 ± 0.002 obtained from a fit of the $[\Theta]_{222}$ versus T data for the heptapeptide, Ac-AHAAAHA-$CONH_2$, cross-linked with a_4Ru.[25] In Figure 3, the cross (×) at 0 °C shows the ellipticity expected for $\upsilon_{35} = 0.009$. At the high fractional ellipticity of the ET peptide, relatively large changes in $(\upsilon_{35})^2$ produce small changes in $[\Theta]_{222}$. Therefore, small systematic errors in $[\Theta]_{222}$ will produce large changes in $(\upsilon_{35})^2$. It is also evident that while the fit of the modified Lifson−Roig model to the temperature dependence of $[\Theta]_{222}$ is reasonable, it is not perfect. Systematic deviations of the fit above the data at low temperature and below the data at high temperature are observed. In general, the temperature dependence of $[\Theta]_{222}$ is fit with a homopolymer model which assumes that all amino acids have the same propagation parameter.[26,31,32,37] Deviations of the fitted curve from the data of the magnitude observed here are typically seen in these analyses.[26,32,37] However, by using a heteropolymer model in Figure 3 (individual propagation parameters for each amino acid), the fit to the shape of the curve is better than with a homopolymer model.[26] Deviations between the fit and the data for the temperature dependence of $[\Theta]_{222}$ have been attributed to the assumption that ΔH for helix formation is constant with temperature.[37] However, recent results indicate that ΔC_p for helix formation is probably very small,[38] indicating that this explanation is unlikely. There are two likely causes for the deviation observed for the fit of our temperature-dependent data. Both relate to the treatment of enthalpy. As is usual,[26,31,32,37] we have assumed a single enthalpy can be used for the temperature dependence of the propagation parameter of each amino acid used in the fit. We have also assumed that nucleation is completely entropic and, thus, the nucleation parameter has an enthalpy of zero. Recent results on alanine-based peptides indicate that these assumptions may be oversimplifications.[38−40] Although additional enthalpy terms could be added to our analysis of the data, the uniqueness of these parameters would be questionable.

The Lifson−Roig model allows the fractional helicity at each amino acid along the sequence to be evaluated. In Figure 4, the effect of the a_4Ru cross-link of histidines 17 and 21 is shown through comparison of the fractional helicity of the cross-linked and un-cross-linked peptides as a function of sequence position. The most profound effect occurs at the C-terminal end of the peptide, where the prenucleating cross-link in the ET peptide compensates for the low helix propensity of the histidines at the C-terminus of the RuBpy

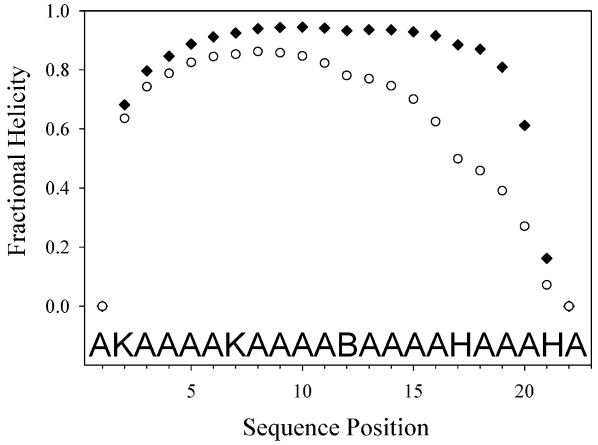

Figure 4. Fractional helicity versus residue number in the ET peptide (◆) versus the RuBpy peptide (○). The fractional helicity at each residue is derived from the partial derivative of the helix-coil partition function with respect to the propagation parameter at each residue position i, $(\delta \ln Z)/(\delta \ln w_i)$, as described previously.[26]

peptide. Most importantly, the average fractional helicity of the amino acid residues between the tris(bipyridyl)ruthenium(II) amino acid electron donor and the first histidine attached to the a_4Ru(III) electron acceptor is increased to 0.92 (92%) from 0.69 (69%) in the un-cross-linked peptide. Thus, in the ET peptide, the medium between the donor and acceptor has a very high helix content.

Electron Transfer Properties of the ET Peptide. The UV−vis spectrum of the ET peptide is essentially identical to that of the un-cross-linked peptide, with peaks at 455 and 286 nm, as reported previously for the RuBpy peptide.[26] The absorption bands of the a_4Ru bis-histidine cross-link have extinction coefficients ~10-fold lower[25,41] than those of the tris(bipyridyl)ruthenium(II) moiety and thus do not contribute significantly to the spectrum of the ET peptide. The near identity of the UV−vis spectra of the RuBpy peptide and the ET peptide indicate that there is little or no direct electronic interaction between the electron donor and acceptor in the ET peptide.

The fluorescence spectrum of the ET peptide is again very similar to that of the RuBpy peptide,[26] with a broad peak centered near 635 nm in water. The full width at half-height of the emission band, $\Delta\upsilon_{1/2}$, is 2530 cm^{-1}, typical for fluorescence emission bands of tris(bipyridyl)ruthenium(II) complexes.[42] Using these data in combination with previously reported electrochemical data for the tris(bipyridyl)ruthenium(II) amino acid ($E°(Ru^{3+/2+}) = 1.22$ 0.05 eV versus SCE)[26] and *cis*-bis(imidazole)tetraammineruthenium(III) chloride ($E°(Ru^{3+/2+}) = -0.086$ versus SCE), we can use eqs 6−8 to calculate the driving force, $\Delta G°$, for photoinduced electron transfer from the tris(bipyridyl)ruthenium(II) excited state, Ru(II)*, to the a_4Ru(III) moiety.[42] In eq 6, $E_D°$ and $E_A°$ are the 3+/2+ reduction potentials of the electron donor and acceptor, and ΔG_{ES} is the free energy of the excited state

(37) Scholtz, J. M.; Qian, H.; York, E. J.; Stewart, J. M.; Baldwin, R. L. *Biopolymers* **1991**, *31*, 1463−1470.
(38) Lopez, M. M.; Chin, D.-H.; Baldwin, R. L.; Makhatadze, G. I. *Proc. Natl. Acad. Sci. U.S.A.* **2002**, *99*, 1298−1302.
(39) Luo, P.; Baldwin, R. L. *Proc. Natl. Acad. Sci. U.S.A.* **1999**, *96*, 4930−4935.
(40) Shi, Z.; Olson, C. A., Rose, G. D.; Baldwin, R. L.; Kallenbach, N. R. *Proc. Natl. Acad. Sci. U.S.A.* **2002**, *99*, 9190−9195.
(41) Clarke, M. J.; Bailey, V. M.; Doan, P. E.; Hiller, C. D.; LaChance-Galang, K. J.; Daghlian, H.; Mandal, S.; Bastos, C. M.; Lang, D. *Inorg. Chem.* **1996**, *35*, 4896−4903.
(42) Roberts, J. A.; Kirby, J. P.; Wall, S. T.; Nocera, D. G. *Inorg. Chim. Acta* **1997**, *263*, 395−405.

Scheme 1

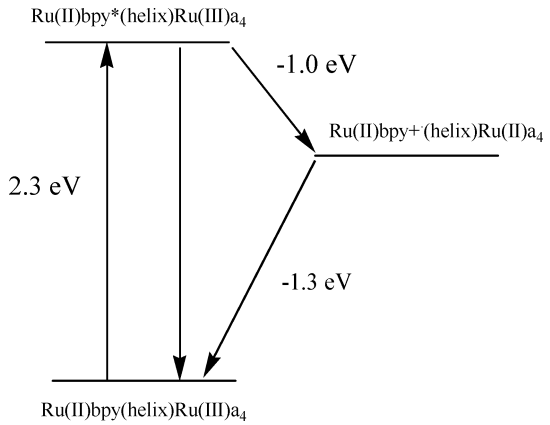

relative to the ground state.

$$\Delta G^\circ = e(E_D^\circ - E_A^\circ) + \Delta G_{ES} \quad (6)$$

$$\Delta G_{ES} = E^\circ + \chi' \quad (7)$$

$$\chi' = (\Delta \upsilon_{1/2})^2/(16 k_B T \ln 2) \quad (8)$$

In eq 7, χ' is the enthalpy due to solvent and low frequency vibrational modes, and E° is the energy difference between the excited state and the ground state derived from the maximum of the emission spectrum ($\lambda_{em} \approx 635$ nm). The results of the calculation are summarized in Scheme 1. The reorganization energy, λ, for this donor−acceptor pair can be estimated with the Marcus cross relation.[43] For the self-exchange reaction of $Ru(bpy)_3^{3+/2+}$, $\lambda = 0.57$ eV.[44] If we use $\lambda = 1.06$ eV for the (bipyridyl)tetraammineruthenium-(3+/2+) self-exchange reaction[44] to approximate the self-exchange λ for the $a_4Ru^{3+/2+}$ histidine cross-link, then λ for our donor−acceptor pair is ~0.82 eV. Thus, we expect the photoinduced ET reaction shown in Scheme 1 to be somewhat inverted.

Photoinduced ET reactions were followed be fluorescence quenching methods at 0 °C in either H_2O or D_2O. Since the emission band for the tris(bipyridyl)ruthenium(II) excited state is at much lower energy than any of the absorbance bands of the a_4Ru moiety ($\lambda_{max} = 310$ nm, shoulder at 286 nm),[25,41] energy transfer is not a possibility for emission quenching for this donor−acceptor pair. Emission decay curves in D_2O are shown in Figure 5. Fits of the data for the ET peptide to biexponential decay curves indicate that a significant component decays with the lifetime of the unquenched donor. In both H_2O and D_2O, a substantial fraction decays with a significantly faster lifetime, consistent with electron transfer quenching. The unquenched portion of the decay curve may reflect peptide, which has lost the a_4Ru cross-link, since such decomposition clearly occurs during laser pulsing in the MALDI-TOF experiments, as described. Lifetimes and electron transfer rate constants are collected in Table 1. It is also possible that there is heterogeneity in the stereochemistry of the a_4Ru cross-link. In our studies on the a_4Ru cross-linked heptapeptide, Ac-AHAAA-HA-$CONH_2$, the major ruthenium product was isolated and characterized. The ruthenium was bound to the ϵ-N of the histidine on the N-terminal end of the cross-link and the δ-N of the histidine on the C-terminal end of the cross-link and shown to strongly nucleate helix formation.[25] Although the ET peptide was isolated as a single peak from a reversed phase HPLC column, it is possible that histidine δ-N/ϵ-N binding isomers are not readily separable. Thus, we cannot rule out the possibility that some heterogeneity exists in the stereochemistry of the $a_4Ru(His)_2$ cross-link in the ET peptide, which could affect nucleation of the helix and thus the coupling pathway, leading to a mixture of species with viable and nonviable pathways. However, on the basis of the observed loss of the cross-link in MALDI-TOF experiments we favor the former explanation.

In both H_2O and D_2O, we observe electron transfer rate constants, k_{ET}, in the range 5×10^6 to 7×10^6 s^{-1} (see Table 1). In a synthetic three helix bundle,[7] a k_{ET} of 4.0×10^6 s^{-1} was observed for photoinduced electron transfer between an excited tris(bipyridyl)ruthenium(II) and a pentaammineruthenium(III) moiety attached to a histidine with four amino acids separating the donor from the acceptor and a similar driving force. No significant tertiary interactions are expected for the shortest pathway between the donor and acceptor in this three helix bundle system.[7] In the ET peptide, four amino acids also separate the electron donor and acceptor. Thus, k_{ET} in a monomeric helix and a three helix bundle are

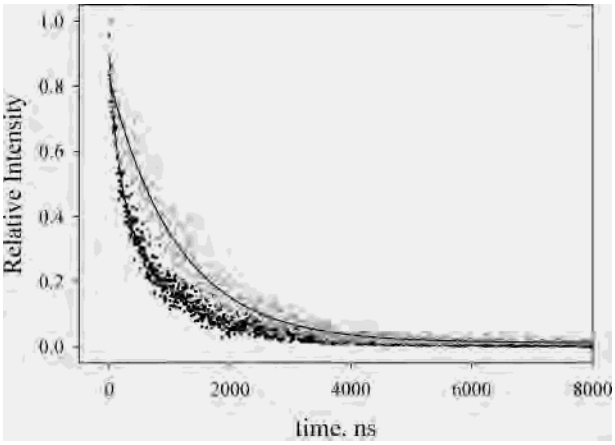

Figure 5. Normalized fluorescence intensity as a function of time for the ET peptide (black dots) and the RuBpy peptide (gray dots) after excitation at 450 nm with a nitrogen/dye laser. Emission was monitored at 637 nm. Measurements were made in D_2O at 0 °C. Samples were purged with Ar for 30 min prior to measurements to remove O_2. The solid lines (—) are fits to a double exponential decay (ET peptide) or a single exponential decay (RuBpy peptide).

Table 1. Lifetime Data for the ET Peptide and the RuBpy Peptide in H_2O and D_2O at 0 °C

solvent	peptide	τ_1 (ns)[a,b]	τ_2 (ns)[a,b]	k_{ET} (s^{-1})[c]
H_2O	ET peptide	634 ± 5 (0.80)	115 ± 36 (0.20)	$7 \pm 3 \times 10^6$
	RuBpy peptide	644 ± 11 (1.0)[d]		
D_2O	ET peptide	1040 ± 42 (0.54)	182 ± 40 (0.46)	$5 \pm 1 \times 10^6$
	RuBpy peptide	1142 ± 15 (1.0)[d]		

[a] Relative amplitude of lifetime is given in brackets. [b] Average and standard deviation for lifetimes are based on 3 or 4 separate trials. [c] The rate constant, k_{ET}, is calculated with eq 6 in the Experimental Section. [d] Data from ref 26.

(43) Marcus, R. A.; Sutin, N. *Biochim. Biophys. Acta* **1985**, *811*, 265−322.
(44) Brown, G. M.; Sutin, N. *J. Am. Chem. Soc.* **1979**, *101*, 883−892.

indistinguishable within error for the same donor−acceptor separation within helical structure.

We carried out electron transfer measurements in D_2O versus H_2O to determine if there is a kinetic isotope effect on k_{ET} in a helical medium.[19] The reorganization energy, λ, in H_2O versus D_2O is not expected to change significantly since the static and optical dielectric constants of these solvents are similar.[45] A dielectric continuum approximation for the solvent reorganization energy[43] indicates <1% difference in the reorganization energy for H_2O versus D_2O. Thus, the Franck−Condon factor in the Marcus equation should be unaffected by changing from H_2O to D_2O. Within error, k_{ET} in D_2O and H_2O are the same (see Table 1). However, the error ranges on k_{ET} are such that an isotope effect of the magnitude reported previously for a carboxylate-bridged donor−acceptor system[19] would be missed in our case.

Since the time constants for helix formation have been reported to be on the ~200 ns time scale,[46] which is similar to the time scale observed for ET in our system, helix dynamics could affect the magnitude of k_{ET}. The main contributor to the 200 ns time constant for helix formation is expected to be helix nucleation. In a prenucleated helix, such as the one reported here, the dynamics of structural perturbation in the helix are more likely to be due to redistribution of helical lengths (i.e., propagation). Redistribution of helical lengths is expected to occur on the 1−10 ns time scale.[46] Thus, dynamics in the ET peptide are expected to be fast compared to the observed electron transfer reaction. When the rates of conformational interconversion are fast compared to rates of electron transfer, the observed electron transfer rate will be a population weighted average of the rates from the different conformational states.[47] For the ET peptide, our modified Lifson−Roig helix−coil model[25] indicates that the helical conformation will be populated ~92% of the time between the donor and acceptor (Figure 4). Thus, k_{ET} from nonhelical conformations will make only a small contribution to the observed electron transfer rate constant.

Given the observed k_{ET} of $7 \pm 3 \times 10^6$ s^{-1} in H_2O and the estimated $\Delta G°$ of −1.0 eV and λ of 0.82 eV for the photoinduced ET reaction, we can evaluate the electronic coupling matrix element, H_{ab}, as in eq 9, where FC is the standard expression for the Franck−Condon factor in the Marcus equation.[43]

$$H_{ab} = \{k_{ET}/(FC)\}^{1/2} \quad (9)$$

We obtain a value of $H_{ab} = 0.19 \pm 0.04$ cm^{-1}. This number can be compared with H_{ab} values available in the literature for cytochrome *c* variants where electron transfer is between Fe^{2+}−heme and bis(bipyridyl)imidazoleruthenium(III) attached to a surface histidine.[48] Using edge-to-edge pathways (edge of bipyridyl ring to edge of histidine imidazole ring) encompassing the best combination of covalent bonds and hydrogen bonds, as used in the cytochrome *c* work, there are 2 best pathways with 10 covalent bonds and 1 hydrogen bond between the donor and acceptor in the ET peptide. In the pathway model,[1,2] the electronic coupling, H_{ab}, is given by eq 10, where ϵ_c, ϵ_H and ϵ_{ts} are the decay factors for electronic coupling through covalent bonds and hydrogen bonds and through space, respectively.

$$H_{ab} \propto \Pi\epsilon_c \Pi\epsilon_H \Pi\epsilon_{ts} \quad (10)$$

For electronic coupling through a hydrogen bond, $\epsilon_H = \epsilon_c^2 e^{-1.7(r-2.8)}$, where *r* is the distance separating the hydrogen bonded donor and acceptor. Using standard helical ϕ, ψ angles (HyperChem release 3.0), the hydrogen bond distance in an α-helix is 3.0 Å, which gives $\epsilon_H = 0.26$. This magnitude of ϵ_H is equivalent to decay through 2.7 covalent bonds. Thus, the shortest edge-to-edge pathway from donor to acceptor in the ET peptide is equivalent to 12.7 bonds. This 12.7 bond pathway corresponds to a tunneling distance, σ_l, of 17.7 Å ($\sigma_l = 1.4 \times n$, where *n* is the number of bonds in the pathway).[1,2] Using the best fit correlation line for log k_{max} versus σ_l for cytochrome *c*,[48] H_{ab} is predicted to be 0.32 cm^{-1} at a tunneling distance of 17.7 Å. If hydrogen bonds are not used in the pathway between donor and acceptor in the ET peptide, the best pathway requires 19 covalent bonds, corresponding to $\sigma_l = 26.6$ Å. Using the log k_{max} versus σ_l correlation line for cytochrome *c*,[48] H_{ab} is predicted to be 0.014 cm^{-1} if hydrogen bonds are not allowed in the tunneling pathway. Thus, the H_{ab} of 0.19 ± 0.04 cm^{-1} obtained for the ET peptide is consistent with hydrogen bonds participating significantly in electronic coupling in an isolated α-helix. This result is consistent with recent data for electron transfer through a monomeric peptide helix studied in organic solvents.[17] Thus, data from isolated α-helices support the involvement of hydrogen bonds in electronic coupling that is apparent from the analysis of data from proteins[1−3] and synthetic three-helix bundles.[7]

Summary

We have prepared a peptide donor−acceptor compound where the donor and acceptor are separated by a short stretch of α-helix. Analysis of the circular dichroism data by a modified Lifson−Roig helix−coil model indicates that the peptide is ~92% helical in the region between the donor and the acceptor. Electron transfer occurs with $k_{ET} = 7 \pm 3 \times 10^6$ s^{-1} in H_2O giving $H_{ab} = 0.19 \pm 0.04$ cm^{-1}. Analysis of the data by a simple pathway model and comparison with H_{ab} values obtained from cytochrome *c* indicates that electron transfer through an isolated α-helix is consistent with the participation of the hydrogen bonds of the α-helix in electronic coupling.

Acknowledgment is made to the donors of the Petroleum Research Fund, administered by the American Chemical Society for support of this work.

IC026166D

(45) Weast, R. C. *CRC Handbook of Chemistry and Physics*, 59th ed.; CRC Press: West Palm Beach, Florida, 1979; pp B-118, B-123, E-61.
(46) Eaton, W. A.; Munoz, V.; Thompson, P. A.; Henry, E. R.; Hofrichter, J. *Acc. Chem. Res.* **1998**, *31*, 745−753.
(47) Hoffmann, B. M.; Ratner, M. A. *J. Am. Chem. Soc.* **1987**, *109*, 6237−6243.
(48) Wuttke, D. S.; Bjerrum, M. J.; Winkler, J. R.; Gray, H. B. *Science* **1992**, *256*, 1007−1009.